

# Buckling along boundaries of elastic contrast as a mechanism for early vertebrate morphogenesis<sup>\*</sup>

Vincent Fleury<sup>1,a</sup>, Nicolas R. Chevalier<sup>1</sup>, Fabien Furfaro<sup>1</sup>, and Jean-Loup Duband<sup>2</sup>

<sup>1</sup> Laboratoire Matière et Systèmes Complexes, Université Paris Diderot/CNRS UMR 7057, 10 rue Alice Domont et Léonie Duquet 75013 Paris, France

<sup>2</sup> Laboratoire de Biologie du Développement, Université Pierre et Marie Curie/CNRS UMR 7622, 9 Quai Saint-Bernard 75252 Paris, France

Received 19 May 2014 and Received in final form 16 January 2015

Published online: 12 February 2015 – © EDP Sciences / Società Italiana di Fisica / Springer-Verlag 2015

**Abstract.** We have investigated the mechanism of formation of the body of a typical vertebrate, the chicken. We find that the body forms initially by folding at boundaries of stiffness contrast. These boundaries are dynamic lines, separating domains of different cell sizes, that are advected in a deterministic thin-film visco-elastic flow. While initially roughly circular, the lines of elastic contrast form large “peanut” shapes evoking a slender figure-8 at the moment of formation of the animal body, due to deformation and flow in a quadrupolar stretch caused by mesoderm migration. Folding of these “peanut” or “figure-8” motives along the lines of stiffness contrast creates the global pattern of the animal, and segregates several important territories. The main result is that the pattern of cell texture in the embryo serves simultaneously two seemingly different purposes: it regionalizes territories that will differentiate to different cell types and it also locks the folds that physically segregate these territories. This explains how the different cellular types segregate in physically separated domains.

## 1 Introduction

The problem of animal formation —especially that of vertebrates— is still largely open. In historical times, it was believed that “Bauplans” (body plans) existed [1] for primitive animal forms. In this view, some form of discontinuous evolution acting at the global scale of the animal body was necessary to explain the formation of the primitive plans (in order to explain the gap between formless tissue and a recognizable animal archetype). Since then, genetics has led to the conclusion that embryo development is controlled by cascades of genetic expressions, especially Hox genes, induced successively as feedback responses to gradients of chemicals [2,3]. The corresponding models are not built on first principles as the origin of the gradients of chemicals themselves remain unexplained, and they also become more and more complex as one tries to model organ or animal development in time and space by gradients of scalar fields [4]. This purely biochemical point of view has recently been challenged by recognizing the visco-elastic nature of embryonic tissues [5] and the

importance of long-range deformations and flow fields in vertebrate development [6]. Simple physical phenomena like buckling, and shearing in rotatory flows [7–9], may play important roles in embryo formation, especially in vertebrates, and provide a mechanism for rapid formation of a body at a global scale. However, while visco-elastic phenomena in biology are often analyzed in terms of continuous media [10,11], living tissue is composed of cells. The coupling between the cellular scale and the mechanical properties of living tissues is an active area of fundamental research [12,13], which has mainly focused on the *Drosophila* model as cell wall imaging is easier in this animal [14]. Visco-elastic movements have been characterized and modeled in the fly [15,16], and discussed within the framework of mechanical models, often with numerical approaches [17].

In the present article, we address the question of how the *cell texture* (cell average size) in the early embryonic tissue might prepattern the animal body and form what may effectively be considered as a “Bauplan”. However, a minimal background is required in order to understand the rationale of the present work.

Animals such as vertebrates form initially a round mass of cells called the blastula [18]. In the case of amniotes (tetrapods that have an egg equipped with an am-

<sup>\*</sup> Supplementary material in the form of thirteen .avi movies and two .pdf files available from the Journal web page at <http://dx.doi.org/10.1140/epje/i2015-15006-7>

<sup>a</sup> e-mail: [vincent.fleury@univ-paris-diderot.fr](mailto:vincent.fleury@univ-paris-diderot.fr)

nios), such as the chicken embryo which will be studied here, this mass of cells is initially almost flat, it has the shape of a disc. This mass of cells next moves and acquires rather rapidly (two days for a chicken) recognizable features of a bilateral animal, with rudiments of head, vertebrae precursors (called somites), flanks, etc. It is a remarkable fact that the morphogenetic movements create a 3D animal which is characterized by different anatomical parts which also play different physiological roles. These anatomical parts are often separated by clear-cut boundaries. For example, at early stages the presumptive spine is separated from the rest of the dorsal area by a furrow, the dorsal and the tail areas are separated from the limb area by another furrow, etc. In amniotes, there is also a clear separation between the embryo territory and the extra-embryonic organs, and even among them, there is another clear boundary separating the amnios from the yolk sac (the digestive extra-embryonic organ of the birds, equivalent to the placenta) [19].

From all these examples we see that cellular differentiation obviously occurs concurrently with morphogenesis and that these two phenomena share common patterns of segregation. This has led developmental biologists to characterize the presumptive territories—including those of the chicken—to try to understand the relationship between the initial cell patterns, their movements, and morphogenesis [20]. Boundaries between cellular domains seem to play an important role in this respect, but it is not at all clear how cellular boundaries relate to the phenomenon of 3D morphogenesis. How does “nature” manage to create animals in which tissues with different physiological (biological) properties are also perfectly organized in physically distinct regions?

To address this question we chose to study the chicken embryo because it is initially almost flat. The first 3D morphogenetic events will therefore obviously consist in forming “folds” on an almost 2D soft plate. These are easier to follow than for frog or fish development where the initial blastula configuration is already 3D. Our hypothesis is that the fold positions are patterned as a result of the differing mechanical properties of the various cellular territories within the blastula. These prepatterned positions are the boundaries between cellular types, such that the folds would naturally segregate the different cell types. As a result, folding of a flat disc would result in a 3D structure with cell territories separated by folds. This would explain the concurrent physical and cell-type segregation characteristic of embryo development.

In order to study this hypothesis, we have strived to image cellular territories during the formation of the animal body in parallel to the fold formation. This requires careful observation of how the cellular features transition from 2D to 3D, and from small scale to large scale. This work therefore relies heavily on zooming in and out of developing embryos in order to correlate the small and large scale features.

The initial structure of the blastula (the thin embryonic cell plate at start of morphogenetic movements) plays a key role in how subsequent developmental events unfold.

We have shown recently that the morphogenetic movements start off on a blastula which has a specific texture, composed of concentric rings, with larger cells at the periphery [21]. Figure 1 (reprinted from ref. [21]) shows the blastula structure, prior to the onset of morphogenetic movements.

We observe cellular domains separating regions of small cells (towards the center), to annular regions of larger cells at the periphery. This, we call a *texture* of cells. The area of larger cells coincides with one ring of cells known as Zona Pellucida, in classical embryology [20], and with the most external ring of even larger cells called Zona Opaca. In the Zona Pellucida cells are thinner and more transparent. In the Zona Opaca, cells are stuffed with yolk (hence their opaqueness). The embryo is composed of two layers, which are delaminated (separated) from the blastoderm, and up to the Zona Pellucida. The substance comprised between the two layers forms a thin circular cavity underneath the central part of the blastula, called the coelom.

The work presented here starts at gastrulation (earlier movements were discussed in refs. [7, 21]), and the purpose of this article is to follow the distribution of cell sizes up to the end of gastrulation and formation of the embryonic folds (this event is known as a “neurulation”), correlate them to embryonic movements, and see how they couple. This is performed by time-lapse video-imaging (See Supplementary Material) following the sample preparation method explained in the Materials and Methods section. An important ingredient is the mesoderm movement, which can be imaged by turning the embryos upside-down. This is why we will present “top” movies showing the behaviour of the ectoderm during morphogenesis, and “underneath” movies, showing the related mesoderm movement.

The text is organized as follows: In sect. 2 we present a number of observations namely: in sect. 2.1 we follow the embryonic tissues from the circular configuration, and up to the onset of fold formation (“gastrulation” stage). We confirm that the structure of rings of cells observed on the upper layer (the ectoderm) is conserved throughout the morphogenetic process.

In a second set of observations (sect. 2.2) we show that the early folding of the ectoderm, with folds parallel to the antero-posterior axis, occurs during the extension of the embryo, and that this early extension of the embryo is caused by the mesoderm spreading under the ectoderm.

In a third series of observations (sect. 2.3) we first show that the rolling-up of the neural folds is the sum of two contributions: initial folds due to antero-posterior stretch, mixed with the medio-lateral<sup>1</sup> active pull of the folds themselves, once they are formed. We also show that folds occur and propagate along or “at” the boundaries between cell territories.

In sect. 3 we present experiments performed on early embryos. In sect. 3.1 we show that the embryo is normally stretched by the vitelline membrane (early stress is ten-

<sup>1</sup> *I.e.* starting from the left and right sides of the embryo, and progressing towards the median axis.

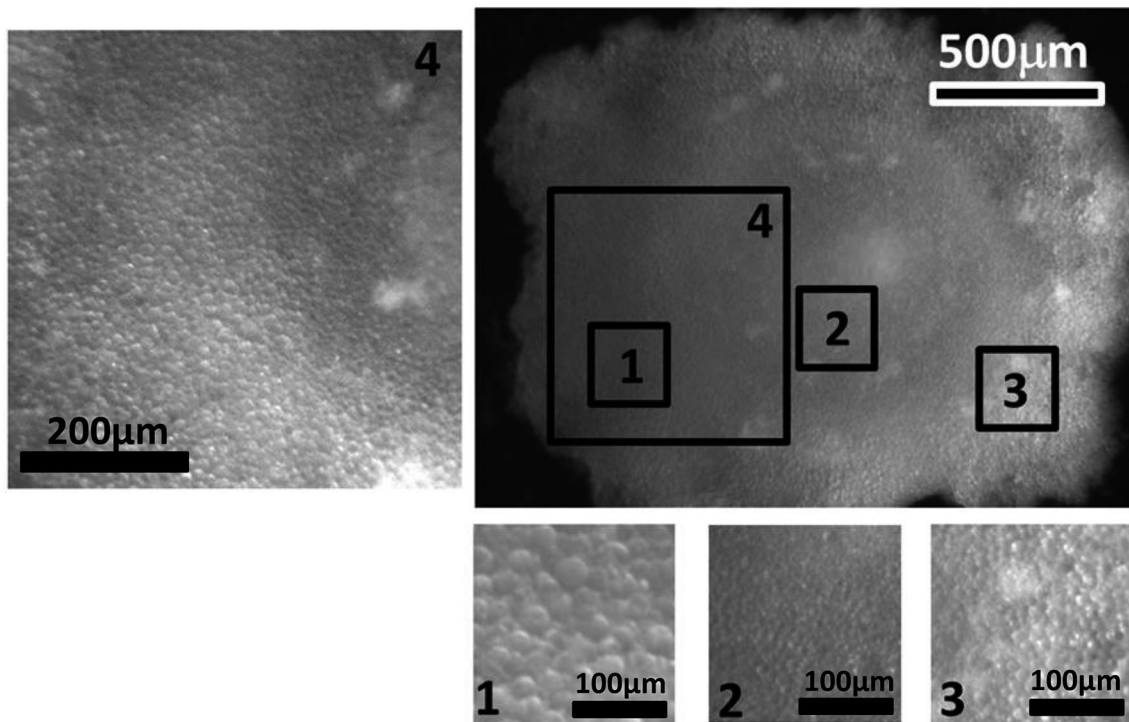


**Fig. 1.** (Adapted from ref. [22]). At start of chicken morphogenesis, the blastula exhibits a structure with the largest cells at the periphery (presumptive territory of an extra embryonic organ, called the yolk sac), a second ring of smaller-sized cells (presumptive Zona Pellucida, another extra embryonic region), and a central disc with the smallest cells (so called blastoderm, presumptive territory of the embryo itself).

sile), and that folds occur spontaneously in the embryo when the embryo is entirely removed from the egg. These folds occur exactly at the boundaries of cell territories, and they anticipate the body form by two days.

In a second experiment, we show that folds can be induced deterministically, by compressing the embryos gently artificially with micromechanical tools (sect. 3.2). Again the folds occur exactly at the boundaries of cell territories. In sect. 3.3 we introduce a small stretch bench, with which we map the deformability of the tissue across the different cell territories. This demonstrates that the contrasts of elastic properties are correlated with the differences in cell diameters.

Having proven that there exists a boundary between cell types which plays a crucial morphogenetic role, we analyze more finely the crossover between cell types, and especially the thickness of these boundaries in terms of cell diameters, in sect. 3.4.

In a final section, we use the stretch apparatus to confirm that the embryo has a simple visco-elastic behaviour at long time scales (sect. 3.5). This justifies the separation of the elastic measurements from the dissipative flow at long time scales.

In the discussion and conclusion section, we explain how the observed contrast of mechanical properties locks the folds of the body, and spatially segregates the embryonic domains.

The work presented here complements and confirms our recent line of work on this question [6,7,21]. Especially, this article provides a confirmation, at cell resolution level, of how the dynamic events are chained, and how the animal body parts are segregated in both 2D (blastula or “convecting” stage) and 3D (neurulation or “folding” stage).

## 2 Results (Observations)

### 2.1 Gastrulation stage

During the first day of development, the vertebrate embryo remains circular and almost static, with visible rings separating cell domains. At the end of the first day the vertebrate embryo starts to involute in a rotatory vortex-like pattern [7,8]. We have imaged the involution of the ectoderm during these early morphogenetic movements. While gastrulation [22] has been studied at a cellular level of detail in *Drosophila* [23], and in anamniotes [24], it has not so far been filmed at cellular resolution in amniotes. Since the chicken blastula is almost 2D, the flow can be imaged with classical optical microscopy, granted the yolk has been rinsed off carefully. The entire blastula is advected in a very slow ( $1\ \mu\text{m}/\text{min}$ ) laminar flow without mixing. Cell trajectories can be obtained by projecting

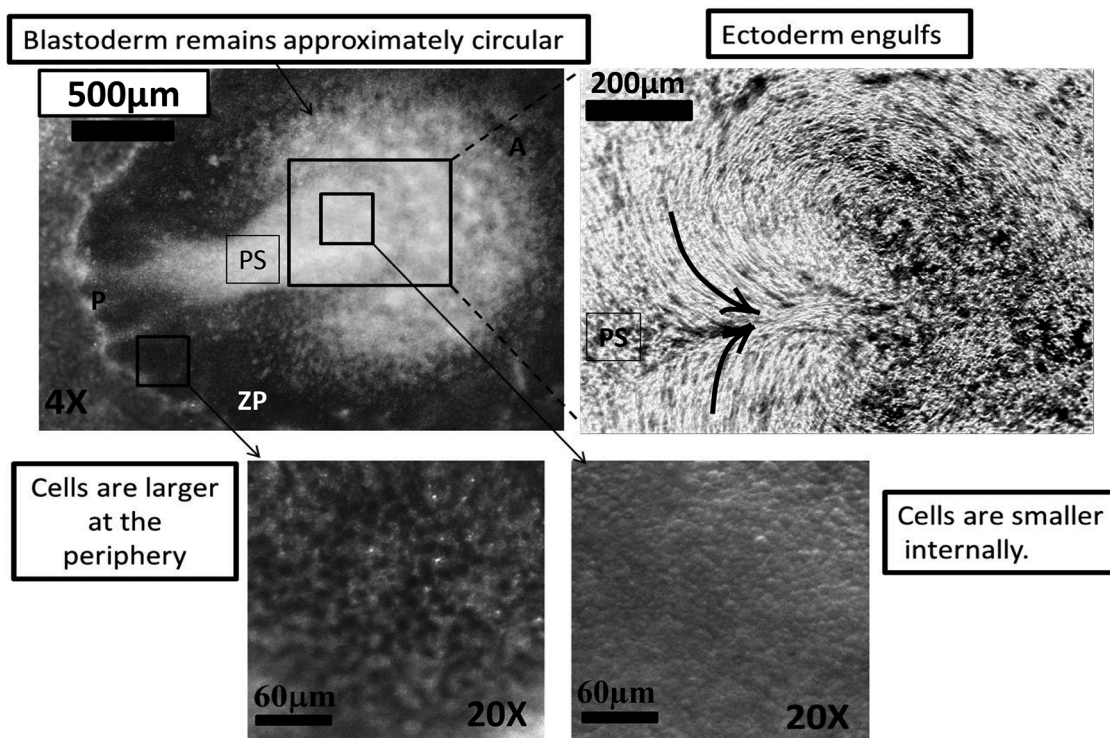


**Fig. 2.** Cell and flow structure in the blastoderm during involution of the ectoderm at cell resolution level (Movie 1 “Early involution in the primitive streak. Magnification 10 $\times$ ”). Cells are larger around the blastoderm than they are inside the blastoderm. Cells at the periphery, belonging to the Zona Pellucida (ZP), are quite flat and transparent (and hence dark in grazing light). Cells in the blastoderm are smaller and denser optically. The blastoderm takes on a horse-shoe shape, which keeps a roughly circular form in the anterior area during the injection of the tissue through the primitive streak. The rotatory nature of the flow preserves the structure of encased annular domains. The trajectories (top right) are obtained by adding frames, subtracting background, and thresholding the image. PS: Primitive Streak. A: Anterior; P: Posterior.

the maximum value of pixels across the stacks (Z-Project tool of ImageJ, courtesy of Wayne Rasband) as the cell nuclei scatter bright spots over a dark field (*i.e.* they serve as flow tracers). Forming the cell trajectories during involution of the cells reveals an involution with a rotatory pattern around the apex of the “Primitive Streak” (PS: the line of involution) (fig. 2). Cell resolved imaging shows that, while the ectoderm is involuting, the structure of encased rings of cells at the outer surface (the ectoderm) is preserved. The ectoderm will later form the embryo body.

The cell configuration at this stage is the following: there are very large cells around the edge of the blastula ( $\varnothing \sim 13 \mu\text{m}$ ), medium-sized cells along the boundary between the blastoderm and the Zona Pellucida ( $\varnothing \sim 9 \mu\text{m}$ ) and smaller cells more internally ( $\varnothing \sim 5 \mu\text{m}$ ), as deduced from a direct cell count within equally sized boxes at 20 $\times$  magnification (see fig. 2, and other figures below).

Direct High Definition photography in grazing illumination by the end of gastrulation evidences 4 main areas (fig. 3): small cells in the presumptive Central Nervous System, medium size cells in the presumptive flank territory (these two zones form the blastoderm), larger cells “far away” in the surrounding extra-embryonic Zona Pellucida, and an opaque ring surrounding the entire embryo, the Zona Opaca.

## 2.2 Chord extension stage

As the process of gastrulation ends, the ectoderm surface undergoes a very strong extension, accompanied, again, by lateral vortices [9]. Movie 2 (“Tissue extension during early stages of chord formation”) shows the onset of ectoderm extension and the progressive stretch which generates the chord. The movie concatenates a 10 $\times$  view, then a 20 $\times$  view, then back a 10 $\times$  view. Cells are resolved. Superimposition of the frames in Movie 2 (10 $\times$ ) shows the trajectories during the Antero-Posterior stretch, with a saddle-point located ahead of the primitive streak (fig. 4(A),(B)).

The embryo is pulled apart in both the Anterior and Posterior directions, as if stretched. The 20 $\times$  magnification, at cell resolution level (see Movie 2), shows no observable cellular intercalation during the extension of the axis, giving support to the notion that the embryo is pulled by the mesoderm underneath (additional movies are available upon request). Intercalation would appear as interdigitating cellular rearrangements along the median axis, forming strict alignments contributing to elongating the median axis by cell shape anisotropy. Such rearrangements are not seen during the phase of the extension described here. Another piece of evidence is that the tissue form-

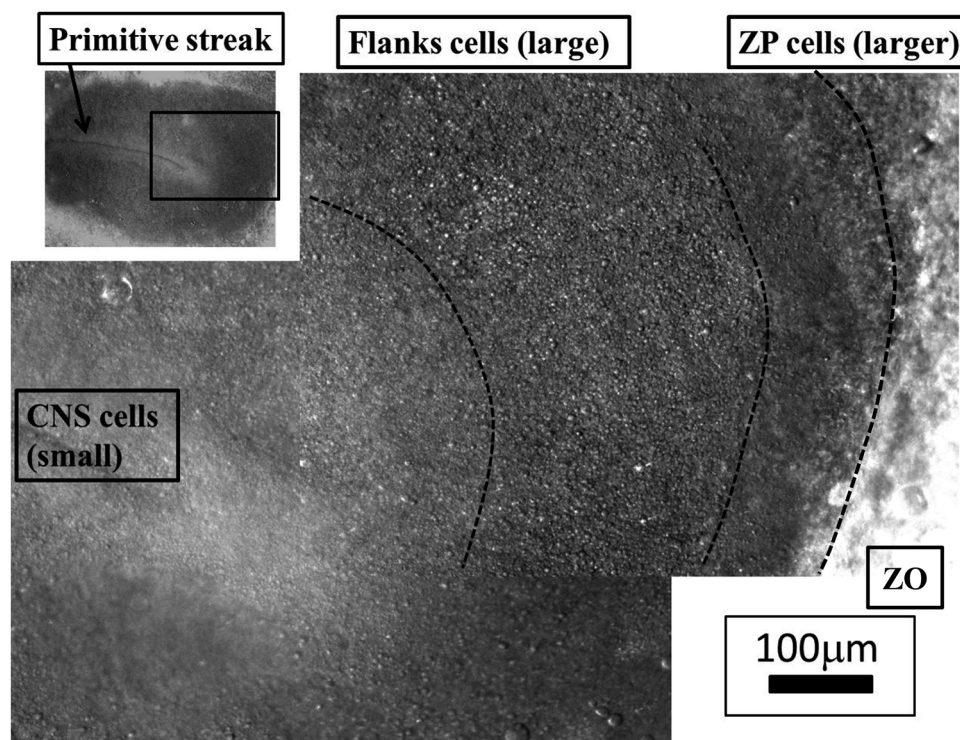


**Fig. 3.** A 10 $\times$  magnification of the blastula formed from a montage of two photos (same embryo), showing the cell dimensions from the primitive streak all the way up to the Zona Pellucida (ZP). The Zona Opaca (ZO) is the final ring which surrounds the entire embryo. Cells are small in the area of the primitive streak where the Central Nervous System (CNS) will form. They are larger in a ring located between the Primitive Streak and the Zona Pellucida, where the body flanks and limbs will form. In the ZP cells are very large.

ing the chord tends to become thinner in the central part in a direction perpendicular to the axis of elongation as would be expected for a material under the influence of a uniaxial stretching force (fig. 4(B)).

Figure 4(C) shows the pattern of displacement during the Antero-Posterior stretch, as measured by Particle Imaging Velocimetry along the median axis, in Movie 2. We observe that the stretch is exerted between the posterior and the anterior limits of the future dorsal axis. Cells around the anterior and posterior limits move as single blocks. Along the presumptive median axis of the embryo, the displacement exhibits a positive Antero-Posterior gradient corresponding to an elongation, as can be seen in the movies. This is at variance with *Drosophila* axis extension, for which evidence suggests that the axis elongates as a consequence of cells intercalating along the Antero-Posterior axis [25]. Mesoderm behaviour during elongation of the *Drosophila* axis has however not been filmed *in vivo* to our knowledge.

As all observations point to a mechanical stretch exerted from underneath the ectoderm, we generated movies of the mesoderm movement by turning the embryos upside-down, and filming the mesoderm instead of the ectoderm. Movie 3 (“Mesoderm flowing under the ectoderm up to formation of the gut pocket. Mag. 4X.”) shows the mesoderm flow, from early involution until chord extension. In particular, for this movie, we managed to remove

the hypoblast (the underneath layer) by careful dissection with fine forceps. It is remarkable that the mesoderm proceeds to spread and invade the ectoderm surface normally even in the absence of the hypoblast and of the coelom (the fluid in the cavity between the hypoblast and the ectoderm). This proves that the tissue located under the blastula is dispensable for these early morphogenetic movements.

Figure 5(A,B) extracted from Movie 3, shows the movement of the mesoderm up to the time of chord extension. A bi-directional mesoderm movement is observed. As shown in fig. 5(B), a centrifugal flow of mesoderm is observed, escaping and flowing away from the primitive streak. The mesoderm conserves or “propagates” the broken symmetry of the Primitive Streak.

At the moment of chord extension, the movement in the presumptive animal tissue (blastoderm) is an antero-posterior extension, along a direction parallel to the average axis of the mesoderm spread in the preceding minutes. However during extension of the chord, the peripheral area of the embryo exhibits a retrograde movement along the same axis, but oriented in the opposite direction to the extension of the chord. This shows that the extension in the central part of the embryo is obtained via a pulling force exerted at the periphery of the embryo: according to the principle of action and reaction, in order to pull the chord across the blastula outwardly, the mesoderm has to

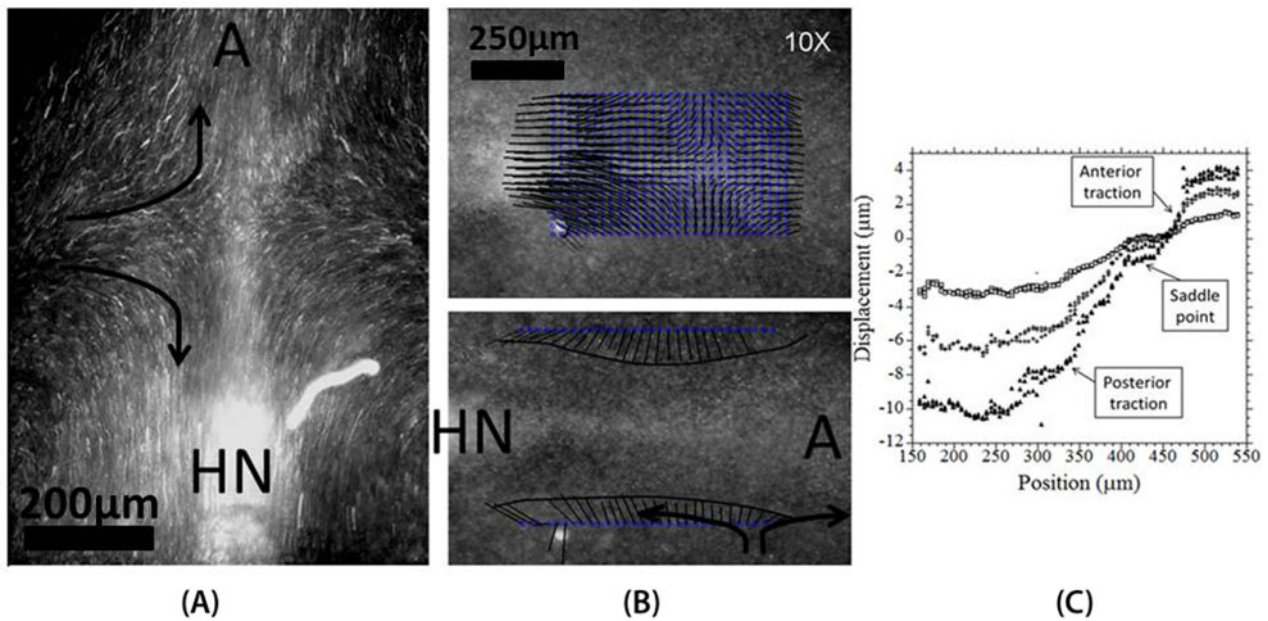


**Fig. 4.** Pattern of Antero-Posterior stretch from Movie 2 at magnification 10 $\times$ . Panel (A) shows the cell trajectories obtained by projecting all frames in the 10 $\times$  stack. The trajectories exhibit an Antero-Posterior movement, with a stagnation point located ahead of the so-called “Hensen’s node” (HN). The orientation in (B) is rotated by 90 $^{\circ}$ -right with respect to (A). Panel (B) shows the movement as analyzed by Particle Imaging Velocimetry (PIV). Panel (B) top shows a hyperbolic flow with a saddle-point. Panel (B) bottom shows the deformation of a reference rectangle showing a thinning in the direction perpendicular to the stretch, as would result from a uniaxial stretch. If the tissue was extending itself out with a high pressure exerted in the central part, the rectangle formed by the reference points in (B) would “swell” instead of thinning. Panel (C) shows a plot of the displacement field analyzed along the median axis. The displacements along the median axis, as calculated by PIV, are plotted as a function of position along the median axis during the Antero-Posterior stretch. The three curves correspond to displacements during three 15-minute time intervals, spanning a total of 45 minutes. The gradient of the displacement in the plots of panel (C) is the deformation. A growing curve corresponds to a stretch, a descending curve to a compression. A plateau corresponds to a neutral displacement, without deformation. The data confirm a bi-directional stretch, which propagates from the posterior and anterior edges of the blastoderm. The tissue is pulled from both ends. Cells along the median axis show no visible sign of alignment nor intercalation at this stage (see Movie 2). A stands for Anterior; HN for Hensen’s Node (presumptive anal area).

grasp the periphery and pull on it inwardly. The fact that the mesoderm reaches the periphery just before the onset of chord extension lends further support to the idea that the stretch force is exerted by the mesoderm.

This, we believe, demonstrates that the source of the initial lengthening of the embryo median axis, is the flow of mesoderm spreading under the ectoderm. This does not preclude however that, at later stages, the chord may also extend “from the inside” by cell intercalation. However, the Primitive Streak fixes naturally the boundary condition for the early mesoderm flow (antero-posterior), while an independent cue is needed if one wishes to explain axis elongation by localized cell intercalation.

### 2.3 Neurulation stage

We now address the exact moment at which the folds form. Movie 4 (“Onset of formation of the neural folds, until first contact of the folds. Mag. 4X”) shows the ectoderm buckling during the Antero-Posterior stretch, followed by the

neural roll-up. Figure 6(A) left extracted from Movie 4 shows a detailed view of the transition from the chord extension to rolling-up of the neural fold (anterior is to the left, posterior to the right). This movie goes up to the first contact of the left and right neural folds (beginning of neural closure). Cells are resolved. This high-definition movie shows that there are two phases in the neurulation process: first a buckling event linked to the Antero-Posterior traction explained in the previous paragraph followed by an active roll-up of the fold. This second step is characterized by a dramatic change in tissue speed in the direction of the median axis (fig. 6(A) right) at the moment when the tissue starts actively rolling-up. We ascribe this sudden change to a favorable adhesion energy of the tissue onto itself. It occurs when the tissue is folded enough that a zone of contact of the tissue onto itself appears (the folds work and pull themselves forward towards the median axis). This zone of contact has been called “apposition zone” in neural embryology [26]. The rolling-up goes to completion when the two folds meet, forming the neural tube.

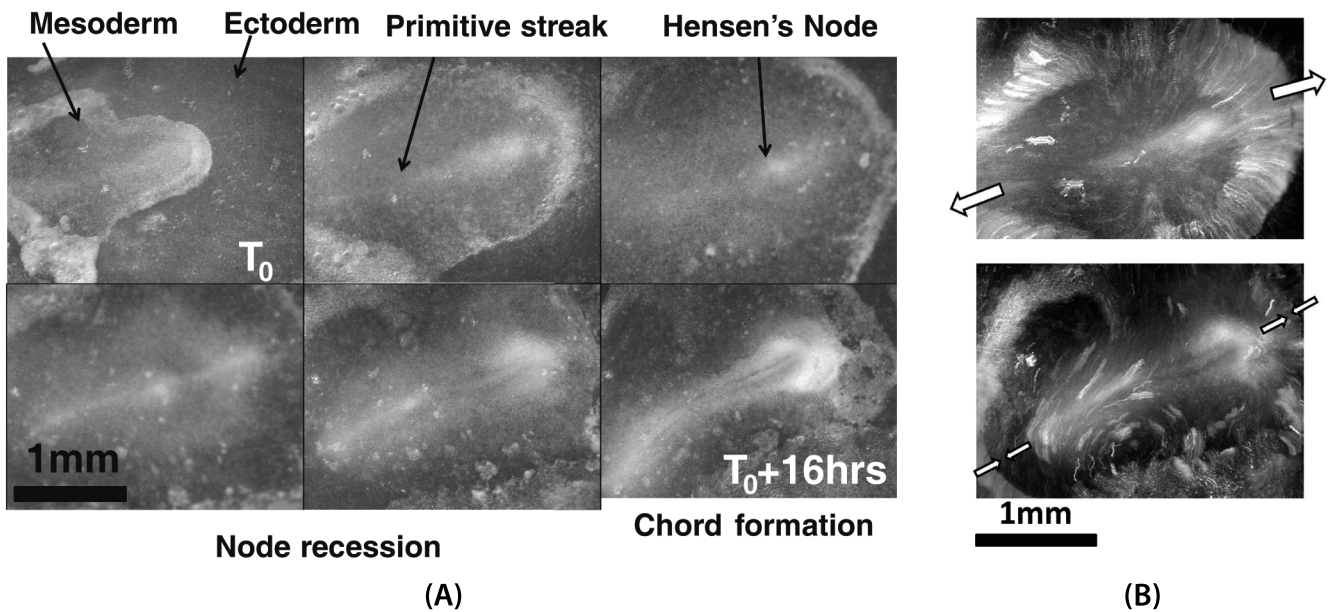


**Fig. 5.** Panel (A), from Movie 3, shows the flow of mesoderm under the ectoderm and the pattern of mesoderm movement during the initial stage of the Antero-Posterior extension. By performing the Z-projection of the frames, the mesoderm movement is revealed: it is observed that the mesoderm moves in an Antero-Posterior pattern. (B) Movement of the mesoderm at the early stage of mesoderm spreading (top), and at the moment of chord extension (bottom). The film confirms that the mesoderm flow has inherited from the Primitive Streak a radial pattern (centrifugal) skewed along the AP axis. Next, the stretch is clearly evidenced as it generates a vortex flow on each side of the chord. The traction along the median axis is well observed. The movie shows that the traction propagates up to the boundaries, where a retrograde movement is seen (by the principle of action and reaction). This retrograde movement of the external contour is particularly visible from the fact that the pointed posterior extension of the blastula (which was out of field) rounds off while it is pulled back inside the field of view.

In fig. 6(B) we show a series of snapshots from the moment of tissue stretch up to the formation of about 6 vertebrae precursors. These snapshots are extracted from Movie 5 (“Formation and propagation of the neural folds until the six somites stage. Mag. 4X.”). We observe that the folds formed on either sides propagate actively as a folding wave, in the posterior direction (which is to the right). The wave segregates the neural tissue from the flanks tissue. Another fold segregates the body from the surrounding Zona Pellucida. Please note that the folds which will eventually give rise to neural tissue actually form at a distance from the median axis, on either side, and are subsequently advected towards the median axis. Movie 6 shows the entire process of chicken gastrulation as *observed from underneath*, until formation of the body folds.

In Movie 5, the folds forming the body “seem” to follow a pre-existing path. The two regions lying on either sides of the groove separating the presumptive neural and flanks territories indeed have different optical densities, hinting at thickness and/or cell type differences (see also Movie 6). During the Antero-Posterior extension and roll-up, which lifts the embryonic tissue in 3D, we observe that the embryo folds along lines which correspond to territories of differing cell dimensions: small cells will form the nervous system, medium-sized cells will form the lateral plates and the limbs, while the large and flat cells will form the surrounding extra-embryonic organs (Zona Pellucida+yolk sac). The embryo folds exactly at the boundaries between these cell types (fig. 7).

These boundaries flow and are dynamically advected during the process (see ref. [27]). The structure of this flow is not that complicated when the phenomenon is followed in detail. Indeed, the observed movement is the superposition of an initial Antero-Posterior stretch (quadrupolar flow) followed by a medio-lateral dipole [27]. This movement deforms the concentric ovals into forms that are progressively narrower in what will be the presumptive “waist” area.

The more central part forms progressively an elongated vertical “peanut” shape, evoking a slender “figure-8”; this area forms the nervous system (CNS), the next “figure-8” forms the flanks and limb plates (fig. 7(A)). One last obvious “figure-8” separates the body from the extra-embryonic territories. The zones are encased like Russian-dolls. Figure 7(A) shows the vortex pattern as calculated at low resolution by PIV tracking. Figure 7(B) shows the vortical flow at cell resolution scale (trajectories are actual cell trajectories obtained simply by projecting frames in a cell-resolved time-lapse movie).

During the physiological folding forming the presumptive Central Nervous System (CNS), the neural folds occur exactly at the boundary between the medium sized and the smaller cells (fig. 7(C)). In fig. 7(C), right, the image shows small cells and medium sized cells in plane, and hence in focus, while the groove of the fold, being more 3D, is out of focus. Movie 7 (“Flow of cell boundaries during propagation of neural folds, Mag 10X.”) shows one hour of advection of the boundary between small cells and medium cells, at magnification 10 $\times$ .

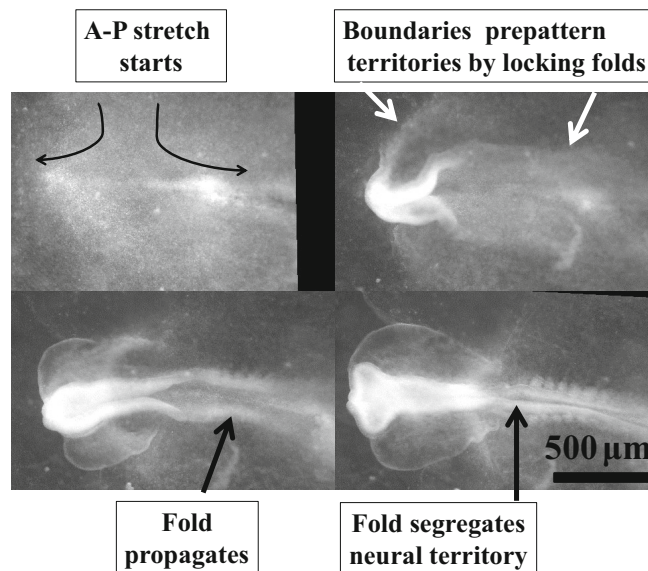
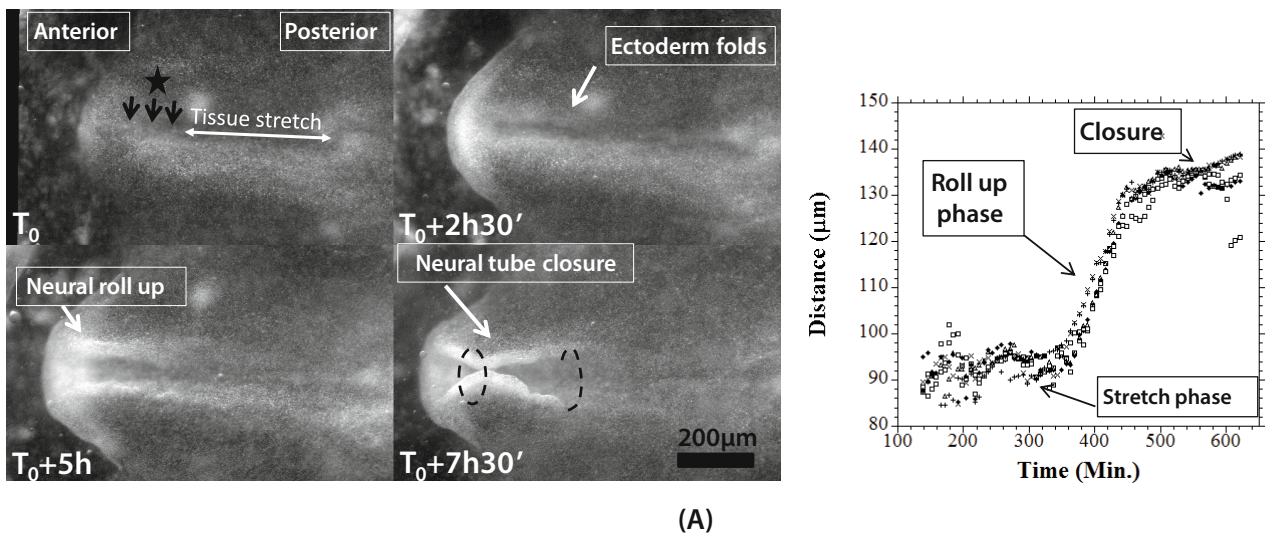


**Fig. 6.** (A) (from Movie 4). Transition from the chord extension stage to the rolling-up of neural crests. The tissue flow (for example at the reference points facing the fold in the area of the black star, and whose movement is followed in the direction of the black arrows) exhibits a discontinuity. The discontinuity occurs at the moment when the active pull of the fold is added to the Antero-Posterior stretch force. To the right, the plot shows the movement (component oriented towards the median axis) of points located in the region of the star shown in the first snapshot to the left. Please watch Movie 4 to visualize the discontinuous roll up of the neural fold. (B) (from Movie 5). The A-P stretch induces the folds, which in turn segregate the territories while they propagate (at this early stage, the mechanism of neural segregation is particularly clear). The fold is locked onto a boundary between tissue domains, recognizable by their optical densities. By the end of Movie 5, the embryo has rudimentary eyes (so-called optic vesicles) and several vertebrae precursors (somites).

These folds form a wave which wraps up around the bottom part of the “figure-8” (fig. 8(A,B)). Figure 8(A) shows the development during formation of the first 10 vertebrae precursors at magnification 4 $\times$ . The snapshots are extracted from Movie 8 (“High Definition movie of embryo body formation up to the 10 somites stage”).

The movie was quickly interrupted to capture images of the cell sizes at mag. 20 $\times$ , which confirms the structure of encased “Russian-dolls”, cellular domains, during the developmental process. Figure 8(B) shows the pattern of extension obtained, by adding frames, resulting from the sum of the Antero-Posterior extension, and the Medio-

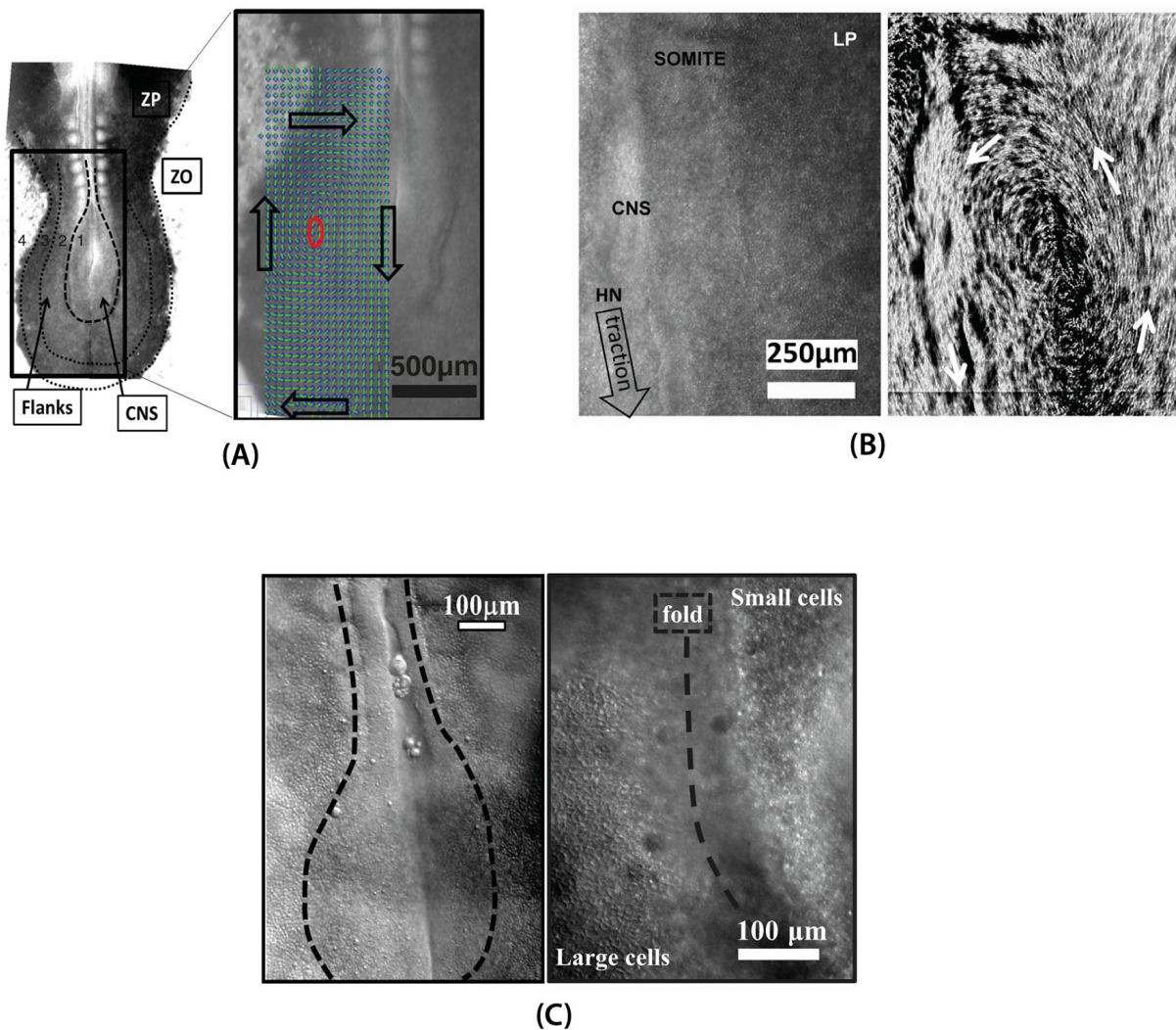


**Fig. 7.** (A). Left: A snapshot of the posterior area, showing the structure of Russian-dolls “peanut” patterns with differentiated zones 1 to 4. The dotted lines correspond to the boundaries between cellular domains 1/2/3/4. The already deformed central area, will form the neural tube; the second area will form the flanks, the next area will form the digestive tract and extra-embryonic organs. The “peanuts” formed by the boundaries 1/2, 2/3, and 3/4 are less slender when travelling from the zone 1 to the zone 4. ZO = Zona Opaca, ZP = Zona Pellucida, CNS = Central Nervous System. Red circle: center of vortex. Right: the vortex movement on the lateral plate of the embryo, as measured by PIV tracking in a low-resolution time-lapse movie. The posterior pull of the tissue generates a fold which propagates downwards “like a zipper”, while it shears the lateral tissue. The result on the lateral tissue is a wide in-plane dipolar vortex movement [6]. (B). Extraction of the vortex pattern at cell resolution level, by direct Z-projection of the cell movements in a time-lapse movie. Panel (B) left shows one snapshot in a movie of embryo development at magnification (10×). The median axis is to the left, the field of view comprises the neural area and a large part of the lateral plate, recognizable by its medium sized cells (to the right). The domains of small cells of the neural area are visible to the left. Panel (B) right shows the vortex pattern as obtained by projecting a time-lapse movie of one hour with the Z-project tool in ImageJ. The lines in panel (B) right are the actual trajectories of the cells visible in panel (B) left. These are obtained in direct white light microscopy, without any staining. In the flanks area (called “Lateral Plate”), the tracks reveal a very coherent (laminar) movement with persistent cell tracks (no Brownian crossing of cells). ZP stands for Zona Pellucida; NS for Central Nervous System; LP for lateral Plate; HN for Hensen’s node. (C). The fold between the medium-sized cells and the smaller cells, is locked exactly over the boundary between cell types (left, snapshot 10×, right 20×). The early stage of the folding process is recognizable in the 20× snapshot by the fact that the tissue forming the boundary between cell types is out of focus (the fold is “going down”), while the smaller and medium cells are in focus. The fold propagates dynamically (Movie 7).

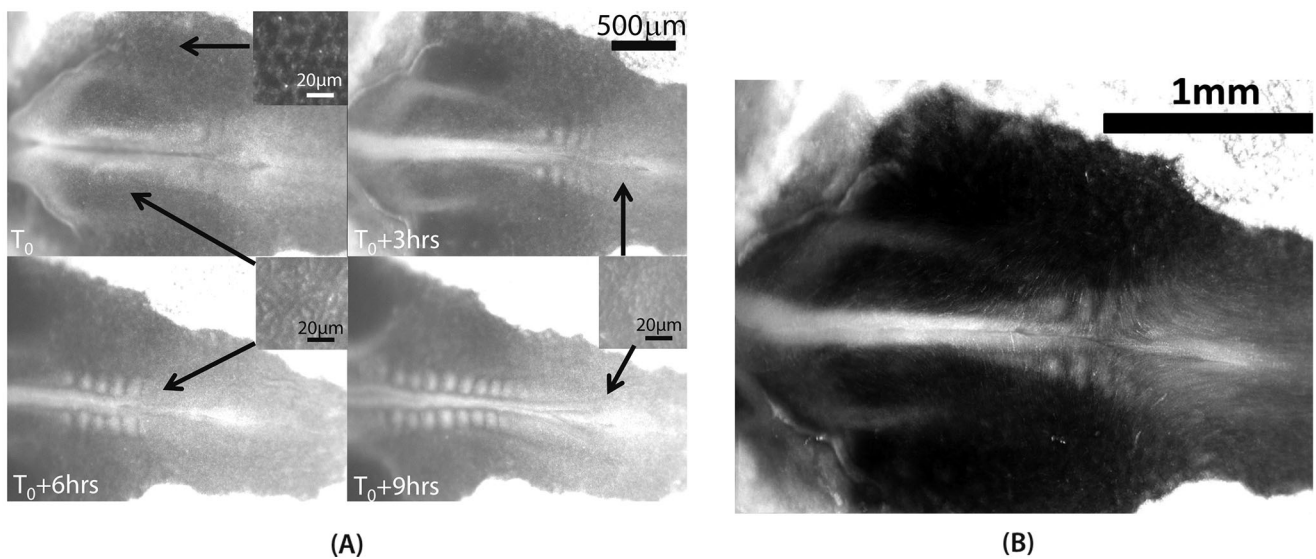


**Fig. 8.** (A). From Movie 8. Montage of four stages of the extension during formation of 10 somites, with cellular detail in the three main zones: extra-embryonic organs have large cells; flanks have medium-sized cells; neural territory has smaller cells. The folds propagate physically the boundary between cell sizes. (B). Construction of the flow map during embryo development (corresponding to 10 somites of development). By adding frames, one observes the Antero-Posterior extension of the embryo away from a central point. The entire embryo exhibits a quadrupolar movement with vortices revolving over the hindlimb plates due to the posterior traction. The boundaries are advected into the flow.

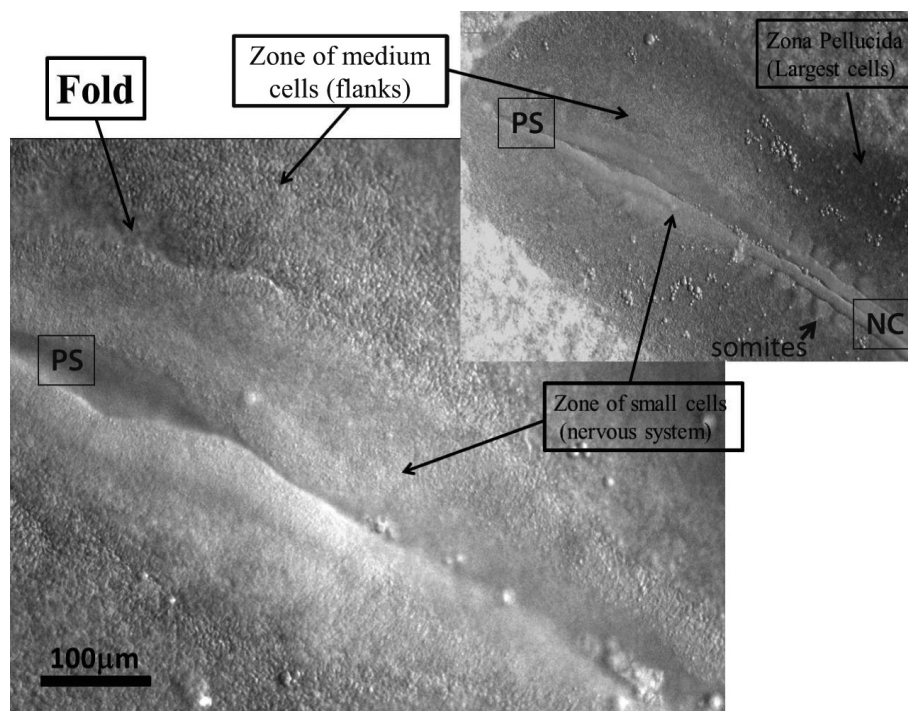


**Fig. 9.** From Movie 9. Dynamic observation of the posterior area of the embryo during completion of the closure of the neural tube. It shows the propagation of the fold between the presumptive nervous system and the flanks. The folds wrap up over the presumptive tail bud area. Movie 9 shows the neural closure first at magnification  $4\times$ , next at  $10\times$ , then again  $4\times$ . Cells are actually resolved in full range view. PS = Primitive Streak; NC = Neural Crest. Somites = vertebrae precursors.

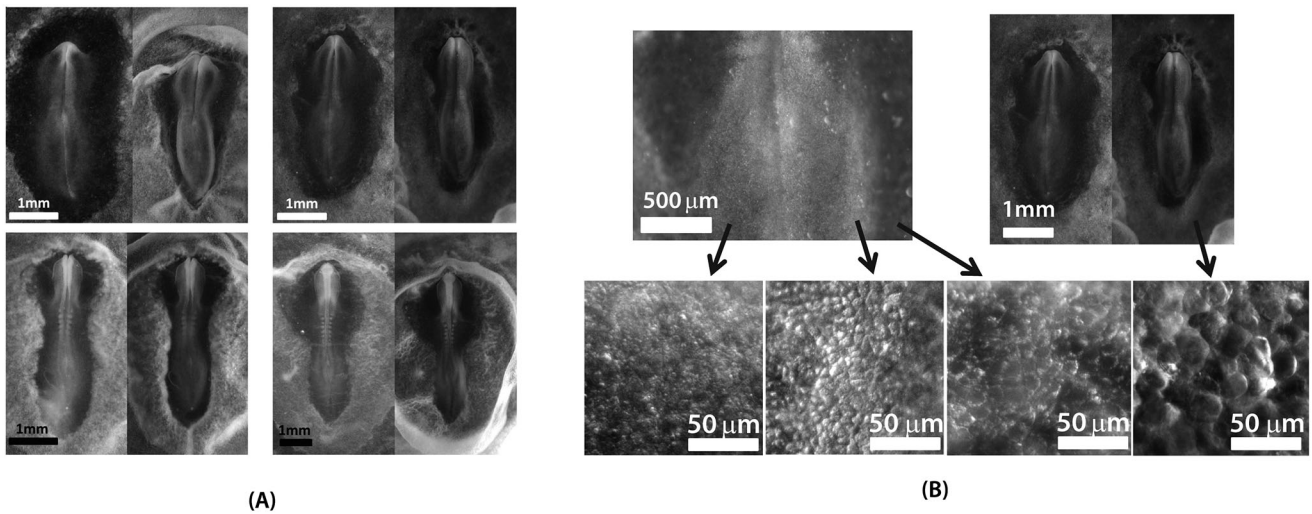


**Fig. 10.** (A): Examples of embryos in an almost physiological stretch (left) and after removal of the embryo from the vitelline membrane and the albumine (right). The embryos systematically buckle along the presumptive flank area in a pattern of “figure-8” that anticipates the body contours. Also, the neural fold deepens. (B). Observation of the cell texture in these spontaneously buckled embryos. Cells are quite large and swollen in the “Zona Opaca” (ZO). They are large and thin in the “Zona Pellucida” (ZP), medium sized in the presumptive flank area, and small in the presumptive nervous system. The folds anticipate the physiological situation. Cell size varies in a surprisingly regular staircase pattern (diameters in the order, 4, 8, 11, 18 micrometers, approximately).

Lateral neural folding. Since both the Antero-Posterior extension, and the Medio-Lateral movements have a saddle-point, a stagnation point remains in the vector field. In fig. 9 we show snapshots from the Movie 9 (“Film of embryo body formation, during the closure of the neural folds, *i.e.* between the 4 and 8 somites stage.”). The film concatenates three sequences generated by changing the magnification from  $4\times$  to  $10\times$ , and back to  $4\times$ . This movie shows in detail the dynamics of the end of the neural crest closure in the posterior area, when the fold wave wraps over the primitive streak and forms the tail bud.

As shown in figs. 7 and 8, the folds are transported in a rotatory movement. The overall movement is the product of an out-of-plane folding and of an in-plane laminar flow of tissue. The fold positions are pre-patterned but still move in the in-plane flow.

We now turn to experiments which aim at proving that the folds which we observe at cell boundaries are locked by the mechanical properties of the tissue.

### 3 Results (Experiments)

#### 3.1 Relaxing the physiological stretch

The egg yolk is naturally stretched [28]. It has long been known that if embryos are removed from the egg, they must be stretched back to resume normal growth *in vitro*. This is the principle of several incubation methods, such as New’s method [29]. The tension of the chicken vitelline membrane has not been measured to our knowledge. This lack of quantitative data for chicken is presumably due

to the fact that the chicken embryo tends to spontaneously stretch itself out when put to incubate on a substrate or on its own vitelline membrane, as explained by New [29]. It is classical knowledge in the poultry industry that the egg membrane softens with time [30] (Supplementary fig. 1). An order of magnitude of the tension in the chicken vitelline membrane by day 3 can be estimated by using Worthington’s equation for sessile drops, as was used historically for estimates of newt ovocyte membrane tension [31, 32]. We take into account the known density contrast  $\Delta\rho$  between albumin and yolk of 0.106 (egg yolk 1.132, egg albumin 1.026). The tension  $\gamma$  is found by the formula  $\gamma = (1/2)\Delta\rho gh^2(1.641)R/(1.641R + h)$ .  $R$  is the maximal radius, and  $h$  the height of the yolk (Supplementary fig. 1). This gives a value for the membrane tension (averaged over 4 samples) in the chicken vitelline membrane during neurulation of the order of  $0.1 \text{ N/m}^2$ .

We now explain how to observe the chicken embryo in a state where the global tension is cancelled. Let us first cut off the vitelline membrane around very young embryos (day 1, stage 7 of Hamilton and Hamburger standardized stages [33]). We transfer the vitelline membrane, the chicken embryo and the albumine to a Petri dish. We gently stir the Petri dish and rinse off the yolk with a pipette. In this situation, the embryo remains partially stretched, because the albumine stuck to the vitelline membrane is an elastic solid that hinders the relaxation of the stress in the vitelline membrane. We take pictures of the embryos in this situation (all embryos to the left in fig. 10(A)), at low resolution with a binocular. In a second step, we remove the embryos from the vitelline membrane and discard with the help of fine tweezers the vitelline membrane along with all of the albumine. We

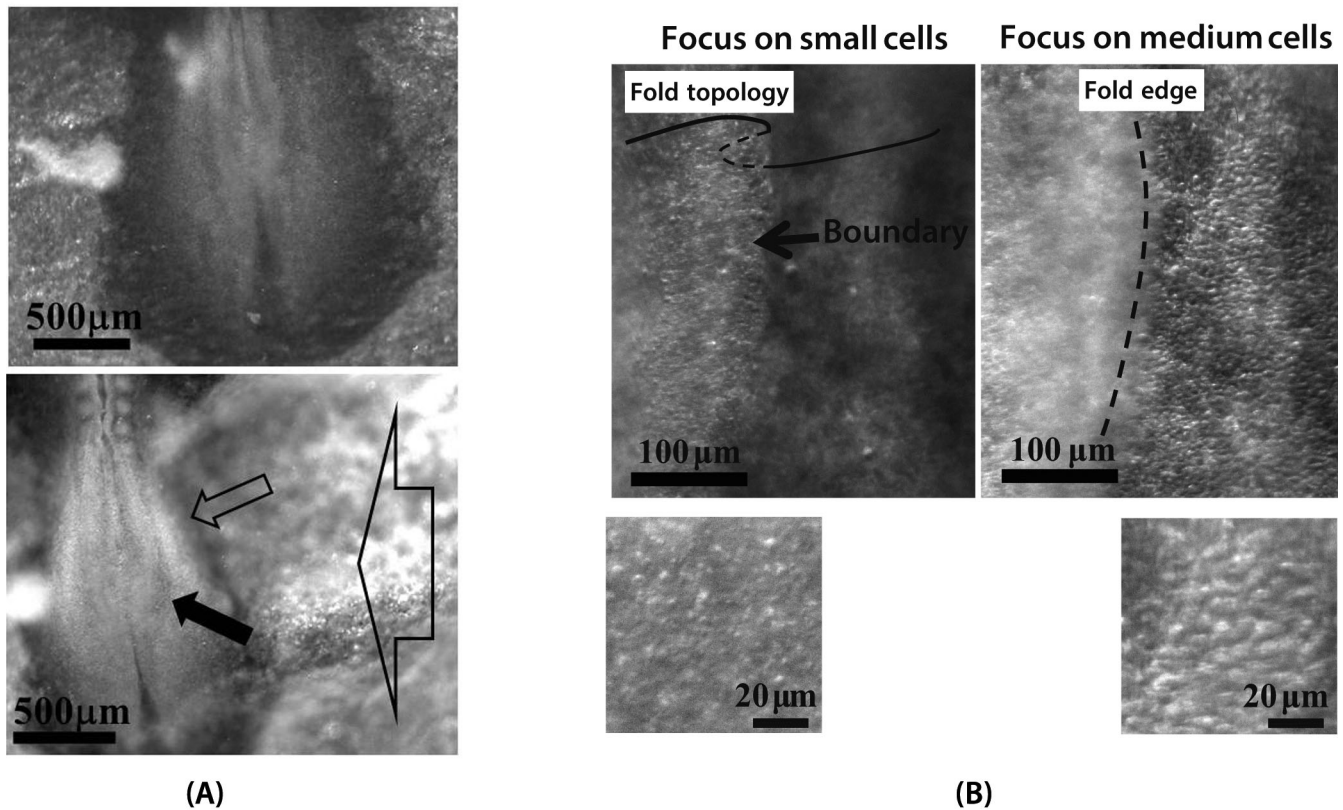


**Fig. 11.** (A). Magnification  $4\times$  of an embryo in the reference and the compressed states showing that the neural fold (black arrow) deepens and progresses, during the compression experiment, while the external contour of the embryo folds (hollow arrow). (B). Higher magnification of the area pointed by the black arrow in (A), in the compressed state, at cell resolved scale ( $10\times$ ). Focusing on the small cells (left), or the medium cells (right), shows that the neural fold is propagated exactly at the boundary between the small and the medium cells. We show schematically the topology of the fold, in order to help the reader. The tissue in the area of the medium-sized cells buckles and slides underneath the area of small cells. Focusing in the plane of the small cells, and in the plane of the medium cells confirms that the small cells area and the medium cells area are no longer in-plane continuously. The boxes show a  $20\times$  magnification in each area.

lay the embryos flat on a glass Petri dish. We now observe that these embryos systematically buckle along the presumptive flank area (fig. 10(A), embryos to the right). We give in Supplementary fig. 2 photographs of all these embryos as observed on their yolk, prior to rinsing of the yolk.

We now transfer the embryos to a higher resolution microscope, and image the cells. We observe that the spontaneous buckling of the relaxed embryo, occurs exactly at the boundary between domains of different cell dimensions. In particular, the body contour appears exactly at the boundary between the medium-sized, and the large-sized cells (fig. 10(B)). Moreover, while neurulation is progressing, we observe on the relaxed embryos that the area where the fold will later propagate, already buckles and that the groove between the prepatterned region deepens exactly along the line forming the prepattern for the fold. The line where the embryo contour spontaneously folds when the stress is relieved is exactly the boundary between medium and large-sized cells, and it is the same boundary where the embryo folds in the physiological case.

The line of fold along the embryo flanks has a pattern of a large figure-8, which anticipates the body contour by two days. Along the median axis in the posterior area, the body axis of the “relaxed” embryos tends to buckle over the plane of the blastula, in a pattern analogous to the tail bud growing over the hind limb territory only two days later (Supplementary fig. 3).

### 3.2 Compressing embryos uniaxially

We investigated the buckling behavior further by compressing the embryos laterally. To do so, we grab embryos with small metallic rakes, and stretch them back and forth (Movies 10-12, many other movies available). We find that embryos that should be flat, systematically buckle along the same line, as if already “pre-patterned” (fig. 11). Figure 11(A) top shows a typical example of embryo in the reference state, prior to a gentle lateral compression, and the compression state is shown in fig. 11(A) bottom. A fold forms which follows the presumptive body contour (hollow arrow), and the neural fold propagates (full arrow). During

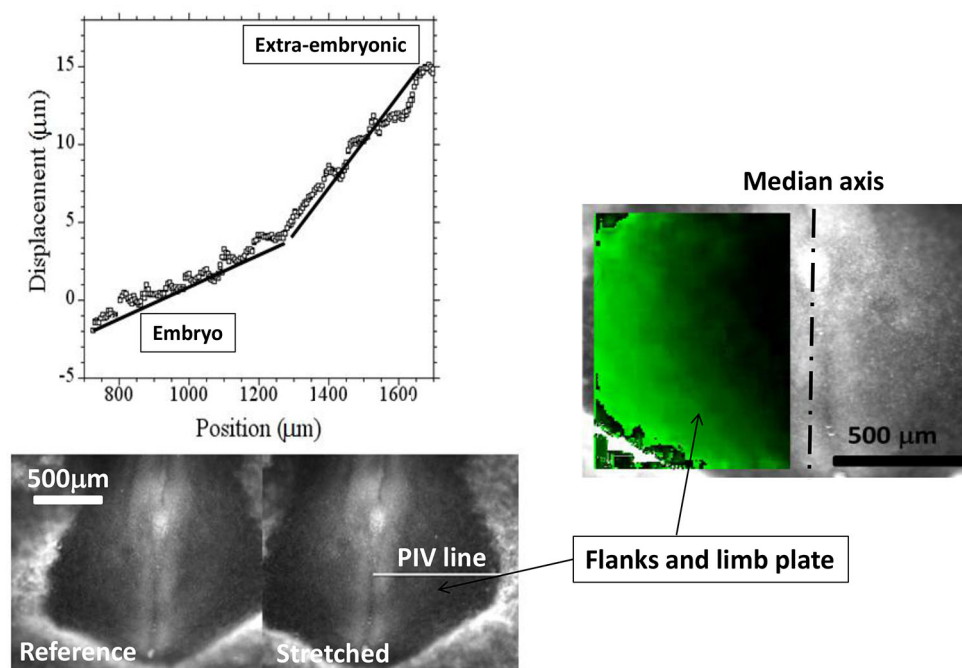


**Fig. 12.** Left: Top left: the graph shows the plot of the displacements in the direction of stretch, as measured by PIV tracking from the median axis and away, in the experiment shown below the graph. The PIV is done between plates in the movie of the stretch experiment, along one line crossing the right half of the posterior area of the embryo; the line used for the PIV is drawn in white on the embryo limb plate. The displacement between the reference configuration and the stretched state is plotted in the graph. The data show a break in slope at the presumptive boundary between the future flanks and future extra-embryonic organs. Right: by calculating point-by-point and color-coding similar data over the embryo picture, an actual map of displacement during the stretch experiment is generated. Such a map is shown to the right, calculated over the left half of the same embryo (the contra-lateral side being shown for clarity). In this experiment, between a reference state and a stretched state, the displacement is zero along the median axis, and  $15\ \mu\text{m}$  at maximum. The elongation pattern reveals the map of stiffness (elasticity  $\times$  thickness) inside the tissue. The elongation is greater in the presumptive zona pellucida, and there exists a prepattern of stiffness which follows the presumptive embryo body (actually readily visible by its optical density).

the compression, the neural fold deepens and propagates in the posterior direction from the already existing neural fold, while the presumptive flank fold appears in the area where it was not yet discernable by eye (several examples are shown in Supplementary fig. 6 at low resolution). Visual inspection shows immediately that the lines where the embryo buckles when compressed with the rakes are exactly the same as the lines where it buckles physiologically or where it buckles when detached from the vitelline membrane: the embryo folds at the boundaries between cell territories.

The fact that the embryo always buckles at the same place shows that this event, far from being random, is robust and “coded” inside the material properties. In simple words: the body of the animal is already *latent*, long before it actually forms.

### 3.3 Measuring gradients of elastic properties

In a third experiment we stretch the embryos uniaxially with rakes (example in Movie 13) and measure the strain along the direction of stretch. The deformation is found to be higher (by a factor 1.5 to 2) in the surrounding Zona

Pellucida than along the median axis and on the lateral plates (fig. 12 left). The Zona Pellucida is therefore much softer. We use PIV tracking to map the deformability in the lower half of the embryo. We find that the line where the embryo later buckles (at this stage the embryo has not yet folded along the flanks) corresponds to the frontier that delineates regions of contrasting deformability (fig. 12 right).

To measure quantitatively the stiffness of the embryo, we used a thin and soft elastic strip glued to a small piece of filter paper that we welded on the embryo (See Materials and Methods section, and Supplementary fig. 7). The elastic strip was pulled uniaxially in the plane of the embryo. The instrument does not measure directly the local Young modulus, but rather the product of Young modulus times thickness. The Supplementary fig. 7 shows typical data plots of deformation as a function of elongation for the elastic strip and for the embryo as measured simultaneously by PIV. For the embryo we measure first the deformation in the presumptive flank area and in the surrounding Zona Pellucida. From the calibration of the elastic strip, we deduce the deformation *vs.* tension in these two zones of the embryo (fig. 13). We find a linear elastic behavior for the embryonic tissue up to 30% strains—for

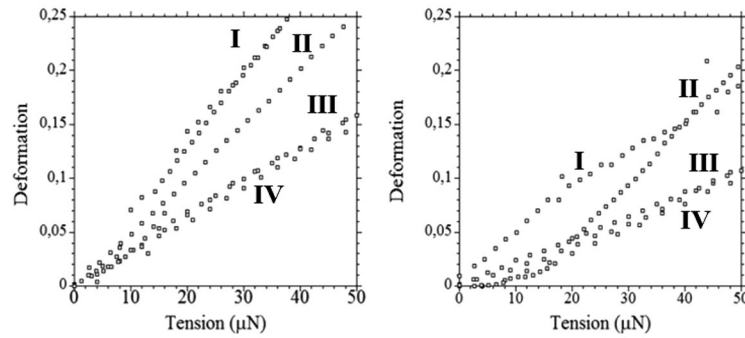


**Fig. 13.** Quantitative measurement of the deformability of the embryonic tissue, by uniaxial stretch. Left panel shows the deformation of the embryo in the extra-embryonic area. Right panel shows the deformation in the presumptive embryo body for 4 different embryos. The data shows a linear behavior at low strains (total deformation  $< 0.05$ ), with a difference of slopes between the two areas which averages 50%.

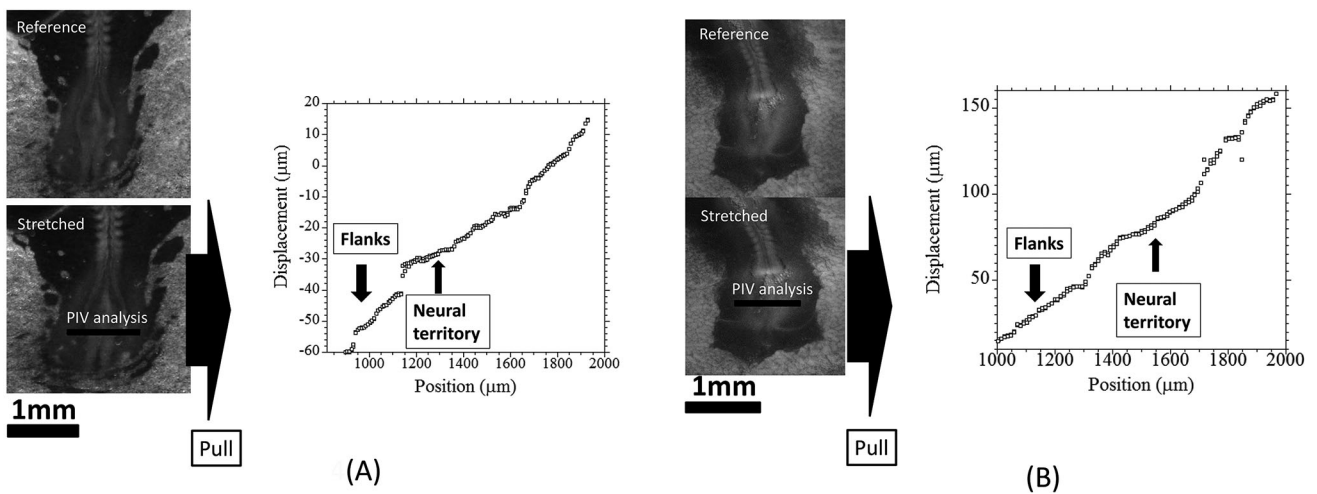


**Fig. 14.** Examples of stiffness contrast in embryos at the 4-somites stage. The data show the displacement along the black lines, as a function of position. The deformation is the slope of the data in the graph. The stretch assay clearly reveals a stiffer zone along the median axis, where deformation is much smaller. In addition, there is a shoulder between the soft area and the stiff area. Panel (A) shows a top view of an embryo stretch assay, while panel (B) shows an underneath view (the embryo is turned upside down), exhibiting similar behaviour (a stiffer area along the median axis while the neural folds propagate).

embryos having 3 to 6 somites (corresponding to Hamilton and Hamburger stages 7 to 10 [33]). The data further confirm at a quantitative level the existence of an elastic contrast between the Zona Pellucida and the presumptive flank and limb area. The line along which the embryo body folds and get segregated from the surrounding extra-embryonic organs are therefore characterized by a sharp contrast of stiffness.

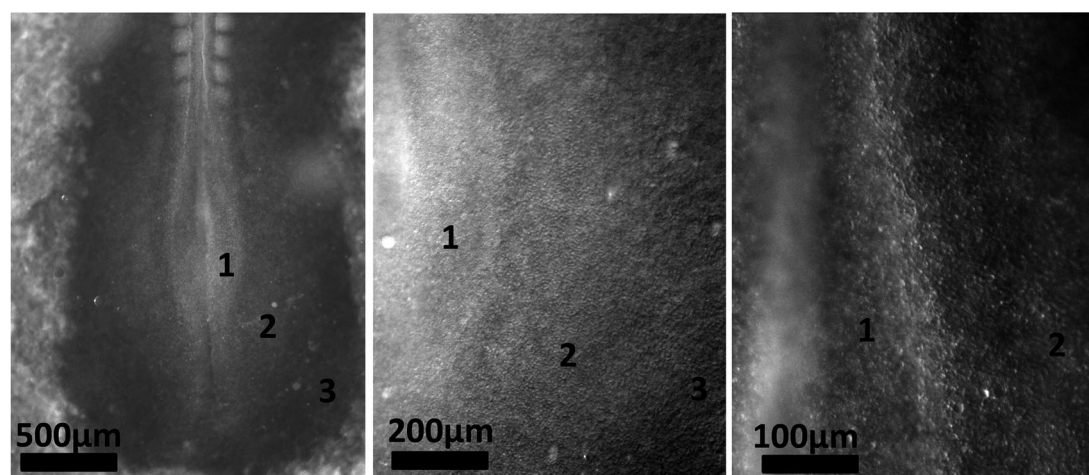
Quantitatively, a force of approximately  $2\mu\text{N}$  is necessary to stretch the embryos at a deformation of 5%. Assuming a thickness of  $200\mu\text{m}$  for the embryonic tissue, (GEISHA data base [35]), we find a Young modulus of  $\sim 200\text{Pa}$ .

We next measured the contrast of stiffness between the presumptive neural territory, and the surrounding flank area. This is somewhat more challenging, in that the fold segregating these two territories occurs rapidly during convergent-extension of the embryo, and one ought to measure these material parameters while the embryo is

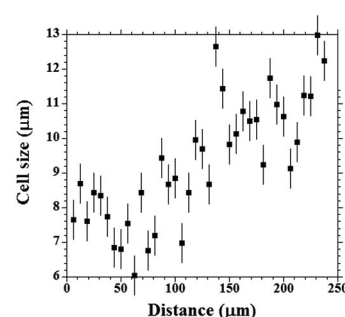
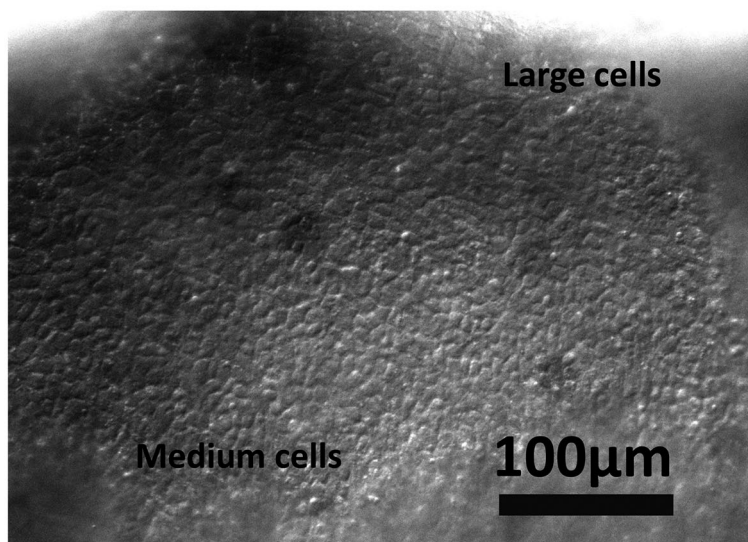
still almost flat along the median axis, before the folds have propagated. Also, the stiffer area is narrower than the flanks or the extra-embryonic organs. Careful observation of the development leads to selecting embryos at the 4 somites stage, and to perform the measurement in a region posterior to the position reached by the closing neural folds, *i.e.* in the area close to the apex of the primitive streak (see fig. 14). Two typical results are shown in fig. 14. This confirms that the propagating neural folds follow a line of elastic contrast between the stiffer median axis and the softer flank area.

### 3.4 Estimation of boundaries thicknesses

A natural question is how sharp are the boundaries between cell territories. It is very difficult to image simultaneously the different areas at high resolution since the embryo is not perfectly flat. Also, there is some variabil-



(A)



(B)

**Fig. 15.** (A) Large field view of an embryo showing the 3 zones. The small cells/medium cells boundary is sharper than the medium cells/large cells boundary. The 10 $\times$  image (middle) is given in full resolution in Supplementary fig. 4. (B). Analysis of cell diameters across the boundary between medium and large cells domains (zones “2” and “3” in a typical image as panel (B) left). The data shows a rapid but smooth variation over a distance of approx. 100  $\mu\text{m}$ , corresponding to 10 cell diameters. The average cell size was measured by sliding a slit from the domain of medium cells towards the domain of large cells, and measuring the cell dimensions inside the slit, but only of the cells which could be extracted (the actual number of cells on which the average is calculated is therefore not uniform).

ity among embryos and in the preparation of samples. Figure 15(A) shows an embryo flank in which the 3 areas could be reasonably imaged in the same snapshot at 10 $\times$  magnification (we give in Supplementary fig. 4 a full-range copy of 15(A)-Middle). It shows that the small cells/medium cells boundary is very sharp. However we were not able to measure quantitatively the thickness of the boundary itself, the cells being too small to be seg-

mented properly over such a small distance; fig. 15(A) right, suggests a thickness of the order of 3 cells.

Figure 15(B) shows the boundary prior to buckling for the medium cells/large cells boundary. Cells are large and sharp enough to be counted.

A direct count of cell diameters in fig. 15(B) across the boundary shows that the boundary between the medium-sized cells and the larger cells is smoother than the small

cell/medium cell one. The boundary between the flank territory (medium-sized cells) and the extra-embryonic organs (large cells) is about  $100\ \mu\text{m}$  thick, *i.e.*  $\sim 10$  cells thick (fig. 11(B) right), with cells oriented slightly ortho-radially.

For the sake of completion, we also imaged by shadowgraph the whole embryo at the primitive streak stage, which reveals that the surrounding gigantic cells stuffed with yolk form a pattern of rough hills surrounding the Zona Pellucida (Supplementary fig. 5).

### 3.5 Long-term behaviour of the embryos under elongational stretch

In the previous section, we have shown measurements of the elastic properties of the embryo. It has been suggested repeatedly that living tissue at such early stages is a viscoelastic material [5, 6]. This explains in general terms how a transient elastic deformation may progressively become irreversible by dissipation. To confirm that the embryo has a visco-elastic behaviour, we performed long time scale stretch experiments on the embryos. The experiment consists in stretching rapidly the embryos ( $< 10$  sec), and then following the relaxation of the force in the pulling instrument at constant deformation. We observe an almost exponential decay of the stress corresponding to a genuine visco-elastic behaviour of the tissue (here we mean the entire tissue in series, since the elongation bench pulls on the entire embryo) (Supplementary fig. 8). The typical force relaxation time scale is 10 min. This confirms that the embryo tissue dissipates stress just as a soft visco-elastic gel would. This justifies the rationale of the mechanical measurements performed above since the stretch experiments were performed well below the minute time.

## 4 Discussion and conclusion

In a series of articles, one of us has shown that embryogenesis starts by a 2-dimensional visco-elastic vortex flow in thin films [7]. The work presented here describes how the visco-elastic flow continues up to the formation of the 3D outline of the animal. The mesoderm involutes first through the stagnation point of the 2D vortex flow. Then it spreads under the ectoderm. During spreading, an Antero-Posterior stretch force is exerted on the ectoderm (figs. 4 and 5). The global pattern of force acts in the Antero-Posterior direction simply because the boundary condition for the spreading of the mesoderm is the Antero-Posterior directed Primitive Streak.

The stretch exerted by the mesoderm stirs and deforms the annular domains of cells (fig. 7). The boundaries between cell types acquire large “peanut” or figure-8 shapes. Buckling along these cellular boundaries generates a folded surface which is recognizable as the global pattern of the animal (figs. 6, 7, 8). One fold segregates the

neural tissue from the flanks, another fold segregates the flanks from the surrounding extra-embryonic organs.

The folds propagate actively after being triggered [27], and they complete the formation of the dorsal area of the animal body (fig. 8(C)).

The crucial issue in this mechanism is that the *same* lines which serve as domain boundaries for regionalization of different cellular types also serve as domain boundaries for the folding modes (and they also localize forces [27]). The contrast of stiffness (figs. 12-14) is sufficient to lock the folds (fig. 12, and Supplementary fig. 6). This contrast may result either from a gradient of local thickness or from an intrinsic difference in material properties.

Once the folds have formed, the sheet-to-sheet contact in the “apposition zone” [26,27] accelerates the closing process of the neural tube by what may well be a favorable work of adhesion of the ectoderm tissue onto itself. We plan to measure these forces accurately in the near future with our traction bench.

Buckling is a non-linear phenomenon with a threshold that depends on bending modulus (which is in turn proportional to the elastic modulus and moment of inertia). It will therefore occur sooner in the softer area. We may mimic what is happening in the embryo by sticking a sticker (paper tag) onto a rubber foil (fig. 16(A)). This makes a soft foil with a stiffer central domain. We next gently pull the on the rubber foil along the “median” axis. The rubber buckles, and the folds tend to avoid the stiff area and to follow the boundary between the softer and stiffer areas, while the latter rolls up (fig. 16(A)). In a second experiment (fig. 16(B)), we hold and roll up one end of the median axis in a pattern similar to a partially closed neural crest, and gently pull the rubber along the median axis. Thus, we obtain a progressive elastic roll-up of the stiffer area which forms a tube.

The work presented here suggests a simple mechanism for segregating 3D cellular territories by folding, which “automatically” segregates differentiated territories into spatially segregated domains. This mechanism is as follows.

In the case of vertebrate formation, the boundary of the cell mass is initially circular. The progressive accumulation of cell divisions generates Russian-doll-like areas of cells where areas of smaller cells are encased in areas of larger cells. Due to differentiation over time, inside-out molecular gradients, or maybe simply because of mechanical stress [34], internal cells are smaller than peripheral cells. This generates *de facto* a stiffness contrast (the extra cellular matrix being denser). Whenever the surface buckles, it does so along the pattern of rings (possibly deformed by advection). That fixes a few general primitive lines in the animal body, segregating the corresponding territories. These general lines correspond to the overall body plan. Of course, many other biological features will contribute to the exact final form of the animal (we think especially of cell migration which is not considered here).

A natural question is how genetic transcription correlates with the cell domains. Inspection of general data

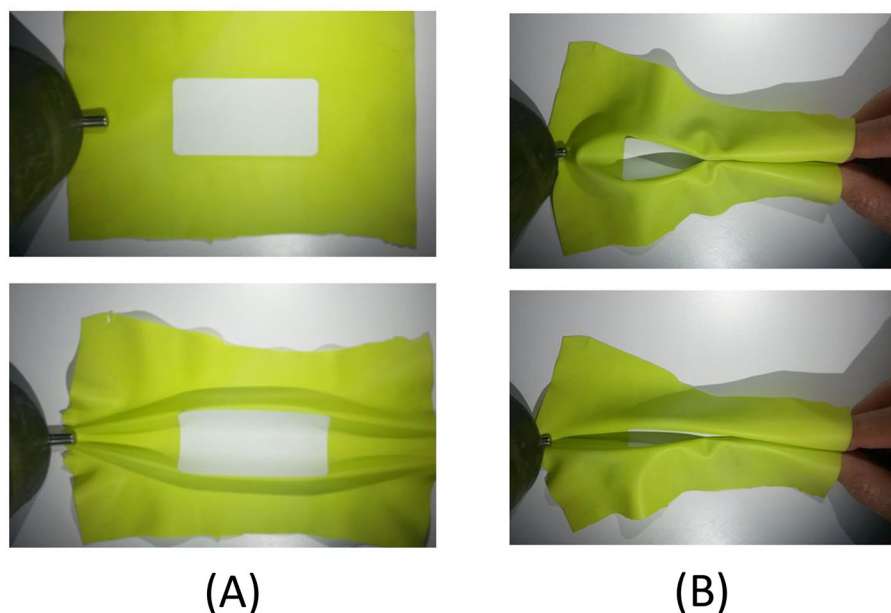


**Fig. 16.** (A) A Proof-of-principle experiment, in which a paper tag is stuck on a rubber foil to create a surface with a stiffness contrast. The rubber foil is held at two points and stretched. The foil buckles as a result but the fold tends to swerve around the central stiffer area. This reproduces the mechanism of fold propagation along the differentiated domains. (B) Next we hold one end in a roll-up situation, and again pull gently on the rubber foil, and we observe a progressive roll up and closure of the central area. These forms are obtained in an elastic regime.

bases shows readily that many genetic markers have domains of expressions sharply correlated to the cell domains evidenced here. Needless to say, the Zona Opaca, which processes the yolk, has a different metabolic role than the rest of the embryonic and extra-embryonic tissue. If we exclude the obvious case of the Zona Opaca, we find in existing databases that many genes such as those of the adhesion molecules Cadherins correlate with the “medium sized cell” area described here (see for example CDH9 stainings at HH stage 5 (Supplementary fig. 9), or CDH1 stainings at HH stage 6 in GEISHA data base [35]). A review of the currently existing literature will be published elsewhere.

In conclusion, we have shown the existence of annular domains of different cell sizes, with cell size increasing step-wise radially. These boundaries form a 2D template for the animal, whose instruction or “coding” is the contrast of stiffness between rings. Since the 2D body plan locks the fold furrows, the animal pattern is robust against minor spatial or temporal fluctuations in the magnitude of the traction force, as typically may occur during embryogenesis.

We leave for further studies several important other phenomena observed in the course of this work: tensions exerted by the folds, feedback of the folding process onto the boundaries of the cellular domains, possible interdigitation of the domains correlating with brain segmentation. A major issue to be solved in the near future is whether the correlation between cell domains, buckling pattern, and cadherin expressions is causal, and if so in what direction.

## Materials and methods

Embryos are purchased from Centre Avicole d’Ile de France and put to incubate in a standard incubator (Thermo) at 37°C. For low-resolution microscopy and stretch experiments, they are prepared in the following way. The shell is first broken and the entire egg transferred to a plastic cup. A piece of vitelline membrane with the embryo on it, is gently cut off from the vitelline membrane with scissors. It is transferred to a Petri dish with a spoon. In the Petri dish, most if not all of the yolk is rinsed away by washing with phosphate Buffered Saline (PBS) and a Pasteur pipette. When the embryo is clean enough, it is removed from the piece of vitelline membrane and attached to the traction tools (PIV tracking requires the solution to be very clean). For low-resolution time-lapse, the embryos may be transferred with the albumin gel and the vitelline membrane to a Petri dish, all of the yolk being rinsed away. With the albumin gel and the vitelline membrane, the embryo will develop normally for 10 to 24 hours.

For high-resolution, cell-resolved microscopy, the embryos were prepared in the following way, which requires a lot of care: the embryos + the albumin gel + the vitelline membrane were removed from the egg, and carefully rinsed (PBS). Next, the sample was turned upside down. The embryo was detached from the gel + vitelline membrane; then, the gel + vitelline membrane was again rinsed until becoming transparent, and the embryo was put back on the vitelline membrane, after being turned upside down. By doing so, the embryo is incubated on the feeding medium which it has in the physiological situation, but

in an orientation which allows one to image directly the ectodermal surface of the embryo, without staining or any fluorescence protocol. Also, a ring of albumin is deposited around the embryo to serve as a sealant. The embryos can also be filmed in the normal physiological situation, under the albumin gel and the vitelline membrane, but the images are not as crisp. A Minitüb incubating plate is put over the embryo, the albumin serving as a “glue”, and sealing the incubating chamber. A copper plate with a central small window is put over the window of the Minitüb incubating plate to prevent condensation and a Schott Fiber lamp is used with dichroic light in grazing illumination. This gives the crisper images shown in the paper. We noticed that the presence of the small copper window around the embryo would contribute to improved contrast. This was ascribed to a fortuitous Schlieren effect caused by diffraction along the edge.

The stretch experiments were done generally under a Leica FZLIII binocular. Following the recommendation of a reviewer, a few stretch experiments were performed under a Nikon Microscope to confirm that the lines of folding and of strength discontinuities coincide with the boundaries of cell domains. The high-resolution cell-resolved time-lapse movies were done with an upright microscope from Nikon, Eclipse, with long working distance 4×, 10× and 20× objectives. For the stretch and compression experiments two instruments were designed. The first one was a system of small metallic rakes simply used for grabbing the embryos and stretching them (as for example in fig. 11). A lighter instrument was designed for force measurements (only tensile force can be measured). It consisted simply of a piece of filter paper attached to an elastic strip. The elastic is prepared by spreading CAF 4 silicon polymer under a glass slide. Next, a thin strip is cut with a thin lancet blade (Supplementary fig. 7(A)).

It is easy by hand to cut thin strips with widths in the range 200–800  $\mu\text{m}$ , corresponding to stiffnesses in the range 0.05–0.02 (deformation) per mN, depending on the sample. The strip is calibrated with a weighing machine in “hanging” weighing mode, by pulling the strip down and measuring the elongation by PIV.

The embryo is put in a large Petri dish, with a stiff rake holding the embryo on one side. The pull is exerted on the other side with the filter paper glued to the elastic strip. The filter paper piece is carefully deposited by hand, as parallel as possible to the embryo body, on the Zona Opaca of the embryo. Next the filter paper is welded by contacting the tip of an electric welder with its temperature set at 300°. The welding consists generally of 5 points of welding, performed very rapidly (3 sec each). Since the Zona Opaca is stuffed with yolk, it adheres immediately to the filter paper when heated locally, likely by coagulation of minute drops of yolk and albumin.

After welding the piece of paper on the Zona Opaca, PBS is added back into the Petri dish so that the embryo and the elastic strip are totally immersed in about 5 mm of solution. The elastic strip is pulled away at a speed of the order of 100  $\mu\text{m}/\text{sec}$  by means of an electric stepper mo-

tor (Newport). The sample preparation and installation is somewhat tedious and delicate.

When the embryo is pulled, two movies are acquired simultaneously, one showing the deformation of the embryo, and one showing the deformation of the elastic strip. The embryo is observed with a fixed Leica Macro-fluo binocular microscope (magnifications 0.6× to 11×, but rarely beyond 4×), while the elastic strip is observed with a more flexible Optem zoom mounted on an all-purpose microscope stand (Mag. 1× to 6×, but generally at 1× or 2× magnification). Two Stingray monochrom HD cameras with resolution 1600 × 1200 are used in parallel with separate monitoring units (Supplementary fig. 7B).

The PIV analyses were done using the “Tracker Module” for ImageJ developed by O. Cardoso at Laboratoire Matière Systèmes Complexes. This module is available on the academic website <http://www.msc.univ-paris-diderot.fr/~vfleury/portailPIV.html>.

This work was supported by the research projects LABEX Who am I?, and ANR Ensinted.

## References

1. C. Darwin, *On the origin of Species by means of natural selection of the preservaton of favoured races in the struggle for life* (1859).
2. M. Mallo, C.R. Alonso, *Development* **140**, 3951 (2013).
3. L. Wolpert, *Principles of Development*, 3rd edition (Oxford University Press, Oxford, 2007).
4. J.D. Bénazet, R. Zeller, *Cold Spring Harb. Perspect. Biol.* **1**, a001339 (2009).
5. G. Forgacs, R.A. Foty, Y. Shafrir, M.S. Steinberg, *Biophys. J.* **74**, 2227 (1998).
6. V. Fleury, *Eur. Phys. J. Appl. Phys.* **45**, 30101 (2009).
7. V. Fleury, *Organogenesis* **2**, 1 (2005).
8. C. Cui, X. Yang, M. Chuai, J.A. Glazier, C.J. Weijer, *Dev. Biol.* **284**, 37 (2005).
9. O.P. Boryskina, A. Al-Kilani, V. Fleury, *Eur. Phys. J. AP* **55**, 21101 (2011).
10. R. Allena, D. Aubry, *Comput. Methods Biomech. Biomed. Engin.* **15**, 445 (2012).
11. I. Cheddadi, P. Saramito, B. Dollet, C. Raufaste, F. Graner, *Eur. Phys. J. E* **34**, 1 (2011).
12. S.A. Sandersius, C.J. Weijer, T.J. Newman, *Phys. Biol.* **8**, 045007 (2011).
13. I. Bonnet, P. Marcq, F. Bosveld, L. Fetler, Y. Bellaïche, F. Graner, *J. R. Soc. Interface* **9**, 2614 (2012).
14. T. Lecuit, P.F. Lenne, *Nat. Rev. Mol. Cell Biol.* **8**, 633 (2007).
15. V. Conte, F. Ulrich, B. Baum, L. Muñoz, J. Veldhuis, W. Brodland, M. Miodownik, *PloS One* **7**, e34473 (2012).
16. B. He, K. Doubrovinski, O. Polyakov, E. Wieschaus, *Nature* **508**, 392 (2014).
17. M.A. Wyczalkowski, Z. Chen, B.A. Filas, V.D. Varner, L.A. Taber, *Birth Defects Res. Part C: Embryo Today: Reviews* **96**, 132 (2012).
18. S. Gilbert, *Developmental Biology*, Chapt. 13, 6th edition (Sunderland, 2000).

19. A. Romanoff, *The Avian Embryo* (The Macmillan Company, New York, 1960).
20. M. Callebaut, E. Van Nueten, H. Bortier, F. Harrisson, J. Morphol. **255**, 315 (2003).
21. V. Fleury, Biosystems, Special issue "Morphogenesis" **109**, 460 (2012).
22. C. Stern (Editor), *Gastrulation, From Cell to Embryo* (University College, London, 2004).
23. Z. Kam, J. Minden, D.A. Agard, J.W. Sedat, M. Leptin, Development **112**, 365 (1991).
24. M. Behrndt, G. Salbreux, P. Campinho, R. Hauschild, F. Oswald, J. Roensch, S.W. Grill, C.P. Heisenberg, Science **338**, 257 (2012).
25. C. Bertet, L. Sulak, T. Lecuit, Nature **429**, 667 (2004).
26. A.S. Romer, R.S. Parsons, *The Vertebrate Body* (Saunders College Pub., Philadelphia, 1986).
27. V. Fleury, Eur. Phys. J. E **34**, 73 (2011).
28. T. Moran, J. Exp. Biol. **13**, 41 (1936).
29. D.T. New, J. Embryol. Exp. Morph. **3**, 326 (1955).
30. D.F. Kirunda, S.R. McKee, Poult. Sci. **79**, 1189 (2000).
31. E.N. Harvey, G. Fankhauser, J. Cell. Comp. Physiol. **3**, 463 (1933).
32. C. Kemball, Trans. Faraday Soc. **28**, 866 (1932).
33. V. Hamburger, H.L. Hamilton, Dev. Dyn. **195**, 231 (1992).
34. B. Shraiman, Proc. Natl. Acad. Sci. U.S.A. **102**, 3318 (2005).
35. GEISHA, Gallus Expression In Situ Hybridization data base, <http://geisha.arizona.edu/geisha/>.